NJC

New Journal of Chemistry

A journal for new directions in chemistry

Accepted Manuscript

This article can be cited before page numbers have been issued, to do this please use: K. S. Sharma, M. Thoh, A. K. Dubey, P. P. Phadnis, D. Sharma, S. K. Sandur and R. K. Vatsa, *New J. Chem.*, 2020, DOI: 10.1039/D0NJ00666A.

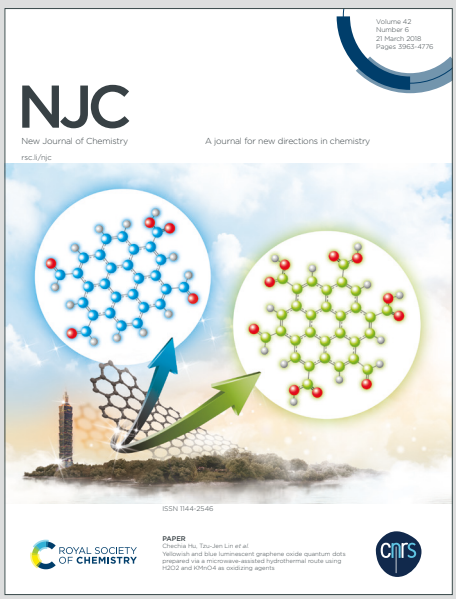

Synthesis of rare earth metals doped upconversion nanoparticles coated with D-glucose or 2-deoxy-D-glucose and their evaluation for diagnosis and therapy in cancer

K. Shitaljit Sharma,[a] Maikho Thoh,[b] Akhil K. Dubey,[c] Prasad P. Phadnis,[a,d]* Deepak Sharma,[b,d], Santosh K. Sandur,[b,d] and Rajesh K. Vatsa[a,d]*

[a] Chemistry Division, Bhabha Atomic Research Centre, Trombay, Mumbai-400 085, India, Email: phadnisp@barc.gov.in, Tel.: +91 22 2559 2229; rkvatsa@barc.gov.in; Tel.: +91 22 2559 2438, Fax: +91 22 2550 5151

[b] Radiation Biology & Health Sciences Division, Bhabha Atomic Research Centre, Mumbai-400 085, India

[c] Bio-Organic Division, Bhabha Atomic Research Centre, Mumbai-400 085, India

[d] Homi Bhabha National Institute, Anushaktinagar, Mumbai-400 094, India

Abstract

Rare earth metal-doped upconversion nanoparticles (UCNPs) are emerging as a new class of biomedical imaging materials due to their higher energy anti-stokes shift, high optical penetration depth and long term repetitive imaging. In the present study, upconversion nanoparticles based on $NaYF_4$ doped with thulium (Tm) and ytterbium (Yb) were prepared by thermolysis method using oleic acid as a capping agent and 1-octadecene as a solvent. The X-ray diffraction pattern of synthesized nanoparticles was found to be matching with the standard hexagonal phase. The nanoparticles were coated with silica using tetraethyl orthosilicate (TEOS) and in order to avoid agglomeration, IGEPAL CO -520 was used as the

surfactant. The coatings of SiO_2 over $NaYF_4$ were confirmed by TEM image and XRD pattern. $NaYF_4@SiO_2$ was further functionalized by addition of (3-aminopropyl)trimethoxysilane (APTMS) followed by either D-glucose or 2-deoxy-D-glucose (2-DG). UCNPs-D-Glucose and UNCPs-2DG were examined for cell viability (MCF-7 cells) by MTT assay. The cellular uptake of UCNPs in MCF-7 cells was seen in terms of emission of blue light form. Further, the uptake rate of UCNPs coated with 2-deoxy-D-glucose was found much faster than that of UCNPs alone under D-glucose starved conditions. The functionalization of UCNPs with 2-deoxy-D-glucose (2-DG) not only increased the uptake of nanoparticles, but also blocked the glycolysis pathway resulting in inhibition of tumor growth as 2-deoxy-D-glucose (2-DG) is mimicking the D-glucose. The results are indicative that these upconversion nanoparticles may find applications in bio-imaging, removal of tumor by precision surgery, therapy and targeted drug delivery.

Keywords: Monodispersed, Upconversion Nanoparticles, Warburg effect, 2-deoxy-D-glucose, Bio-imaging, 980 nm laser *etc.*

1. Introduction

Rare earth metal-doped upconversion nanoparticles (UCNPs) are luminescent bioimaging agents having higher energy anti-Stokes emission formed by sequential absorption of multiple photons through the use of ladder-like energy levels of trivalent lanthanide ions tightly held by an appropriate inorganic host lattice.[1] Generally upconversion process consists of sequential absorption of two or more low-energy excitation photons of NIR light, resulting in the emission of shorter wavelength (*e.g.,* NIR, visible and UV) with the efficiency that is much higher than that of nonlinear multi-photon absorption, under low-cost continuous-wave (CW) diode laser excitation. Use of UCNPs in bioimaging has many

advantageous over the existing fluorophores due to zero auto-fluorescence background which increases the signal-to-noise ratio.[2] Properties like emission with large anti-Stokes shift as compared to the excitation wavelength, sharp emission and high resistance to photo bleaching of UCNPs allow ease and suitable long-term repetitive imaging.[3] Some of the promising applications of UCNPs are differentiating or visualization of diseased area at the time of precision surgery,[4] delivery or release of therapeutic entities to the treatment site[5] and activation of certain compounds like photosensitizer for photodynamic therapy.[6] Utilization of UCNPs for biological applications also included surface functionalization that decides the behavior of UCNPs in biological systems.[7] By carefully choosing the functional groups to be functionalized on the surface of UCNPs, it can be used for diagnosis, treatment or both for many types of human diseases.

Cancer is the major cause of mortality around the globe and the five year survival rate of some of the cancer is just 15%.[8] The poor survival of cancer patients is due to diagnosis of cancer in advanced stage and recurrence after certain period of time.[9] In addition, the techniques used for diagnosis of cancer are expensive and sometimes time consuming.[10] Several techniques are being used in the clinic for diagnosis of cancer. One of the effective techniques is positron emission tomography (PET) where ^{18}F-2-deoxy-D-glusoe (FDG) is used as a tracer.[11] The technique is based on the differential uptake of glucose between tumor and normal cells. Usually tumor cells have elevated glucose uptake than the normal cells, known as Warburg effect. For example, FDG has been taken up preferentially by the tumor cells giving a very bright spot of the tumor region on the image. But this technique has several limitations due to the use of radioisotope.[12]

After diagnosis of cancer, proper treatment modalities are assigned for most of the cases, either removal of the tumoral region by precision surgery is performed, along with radiotherapy or administration of chemotherapy drugs.[13] The major limitation is survival of

resistant cells (cancer stem cells) or leaving behind few tumor cells that can lead to recurrence.[14] To overcome this limitation, strategies which can precisely distinguish the tumoral region should be employed during the surgery. Use of UCNPs functionalized with D-glucose (DG) could be a good strategy as uptake of D-glucose by cancer cells is twenty-fold higher than that of the normal cells.[15] Also, the hydroxyl groups on the surface of UCNPs functionalized with D-glucose can be used to load certain drugs by forming ester linkage or silyl ether linkage.[16]

Considering these facts, we have prepared monodispersed $NaYF_4$ nanoparticles doped with rare earth elements. We noted from literature, various methods have been employed for synthesis of $NaYF_4$ based UCNPs exhibiting versatile applications.[17] Taking synthetic guidelines from literature and optimizing the composition and reaction conditions, we have prepared of Tm and Yb doped $NaYF_4$ UCNPs. They were coated with silica using tetraethyl orthosilicate (TEOS) and followed by functionalization with (3-aminopropyl)trimethoxysilane (APTMS) giving an amine group functionalization on the surface. Analogues of D-Glucose and 2-deoxy-D-glucose (2-DG) were prepared with slight modification of the protocol from the literature. These compounds were conjugated with the amine functionalized UCNPs through amide or thiourea linkage. The presence of D-glucose or 2-DG on the surface of the nanoparticles was confirmed by FT-IR and elemental analyses. The cytotoxicity and uptake studies of the said D-glucose and 2-DG functionalized UCNPs were performed in human breast cancer cells (MCF-7 cell lines).

2. Experimental

2.1 Materials and methods

The chemicals and solvents required for this study, *viz.,* paraformaldehyde, D-glucose, 2-deoxy-D-glucose, yttrium acetate, thulium acetate, ytterbium acetate, oleic acid, 1-

View Article Online
DOI: 10.1039/D0NJ00666A

octadecene, sodium hydroxide, ammonium hydrogen fluoride, IGEPAL CO-520, (3-aminopropyl)trimethoxysilane (APTMS), tetraethyl orthosilicate (TEOS), HBr (33%) in acetic acid, allyl alcohol, silver carbonate, benzoyl chloride, pyridine, zinc metal, ammonium chloride, Dowex 500 resin, lithium bromide, potassium bromide, silver nitrate, potassium thiocyanate and N, N′-dicyclohexylcarbodiimide (DCC), 4-dimethylaminopyridine (DMAP) were purchased from Sigma Chemical Co (St. Louis, MO, USA). Hoechst 33342 was purchase from Molecular Probes Life Technologies (Eugene, OR, USA). Trypsin-EDTA, fetal bovine serum, antibiotic solution and DMEM were purchased from Himedia Laboratories (Mumbai, India). Acetic anhydride was purchased from Spectrochem (Mumbai, India). All other chemicals used in our studies were obtained from reputed manufacturers and were of analytical grade. All solvents were distilled and dried following the standard protocols. The NMR spectra were recorded on the Agilent/ Varian 600 MHz NMR spectrometer with a Unity Inova console operating at 599.88 (^{1}H), 150.84 and (^{13}C{^{1}H}). The ^{1}H and ^{13}C{^{1}H} NMR chemical shifts were relative to internal $CHCl_3$ peak from $CDCl_3$ solvent. The powder X-ray diffraction (XRD) patterns were recorded on a Pan analytical X′pert PRO X-ray diffractometer using Cu-Kα radiation in the 2θ range of 10-70° with step size and time of 0.02° and 1.20 s, respectively. XRD patterns were analyzed by comparing with reported data for the end member compositions (JCPDF files). The transmission electron microscopic (TEM) image was recorded on Libra-120 plus TEM (Carl Zeiss, Germany) operated at 120 kV as the accelerating voltage. TEM images were analyzed by using Image J software taking 100 nanoparticles statistically. For internalization studies, the images of adherent cells were taken using phase contrast microscope (Olympus, Japan). The cytotoxicity studies were performed using a flow cytometer and its results were analyzed using FlowJo software.

2.2 Synthesis

2.2.1 Synthesis of monodispersed $NaYF_4$ nanoparticles doped with rare earth metal ions

The synthesis of the monodispersed $NaYF_4$ nanoparticles was done with a slight modification from the reported literature. Briefly, yttrium acetate (1 g, 3.75 mmol), thulium acetate (64.8 mg, 0.18 mmol), ytterbium acetate (263 mg, 0.75 mmol) were dissolved in a solution of oleic acid (5 ml) in 1-octadecene (30 ml) contained in a three-necked flask under an inert Ar atmosphere. Subsequently, sodium hydroxide (600 mg, 15 mmol) and ammonium hydrogen fluoride (555 mg, 15 mmol) dissolved in methanol were added and heated to 100 °C for 1 h. After methanol was evaporated, a yellow liquid residue was obtained. The residue was further heated to 300 °C with the heating rate of 5 °C per minute. The reaction mixture was heated for 2 h and then cooled to the room temperature. The nanoparticles were precipitated with acetone, dispersed in a minimum amount of hexane and then re-precipitated with acetone. The process was repeated thrice. The obtained nanoparticles were characterized by X-ray diffraction (XRD) analyses, transmission electron microscopy (TEM) and photoluminescence spectrophotometry.

2.2.2 Synthesis of $NaYF_4$@SiO_2-NH_2 ($UCNPs$-NH_2)

Cyclohexane (20 ml) and IGEPAL CO-520 (0.5 g) were added to conical flask (50 ml) and stirred for 15 min. To this solution, UCNPs (20 mg in 10 ml of cyclohexane) were added and stirred for 20 min, followed by the addition of aq. ammonia solution (30 % 500 µl). After stirring for additional 20 min, TEOS (200 µl) was added at an interval of 12 h to 48 h. (3-aminopropyl)trimethoxysilane (APTMS) (200 µl) was added and stirred for additional 24 h. Then methanol (10 ml) was added for phase separation between cyclohexane and methanol. The particles were collected from methanol layer by centrifugation. The particles were characterized with TEM and FT-IR.

2.2.3. Functionalization of UCNPs with D-glucose or 2-deoxy-D-glucose

For the functionalization of $NaYF_4$@SiO_2-NH_2 with either D-glucose or 2-Deoxy-D-glucose, the respective glucose derivatives *viz.,* carboxy glucose *i.e.,* 2-[(2,3,4,6-tetra-*O*-acetyl-D-glucopyranosyl)oxy]acetic acid (*Suppl. Info.* compound **3**) or isothiocynate glucose *i.e.,* 3, 4, 5-tri-O-benzoyl-2-deoxy-D-glycopyranosyl isothiocyanate (*Suppl. Info.* compound **8**) were synthesized and characterized (*Suppl. Info.* Scheme S 1 and S 2). They were further reacted as given below.

2.2.4. Functionalization of amine functionalized UCNPs by D-glucose

To the carboxyl glucose (100 mg) dissolved in dry dimethylformamide (DMF, 5 ml) and treated with DCC (61 mg) for 30 min. at 0 °C, amine functionalized UCNPs were added and stirred for overnight. Catalytic amount of 4-dimethylaminopyridine (DMAP) was added. After stirring for overnight, the UCNPs were washed with acetone and transferred to a round bottle flask, containing aq. ammonia solution (33%, 10 ml). The UCNPs were collected by centrifugation, washed with ethanol, dried under vacuum and characterized with FT-IR and elemental analyses.

2.2.5. Functionalization of amine functionalized UCNPs by 2-deoxy-D-glucose

The 3, 4, 5-tri-O-benzoyl-2-deoxy-D-glycopyranosyl isothiocyanate (150 mg) was dissolved in dry DMF (5 ml) and amine functionalized UCNPs were added. The reaction mixture was heated at 60 °C for 8 h. The nanoparticles were collected by centrifugation and washed with acetone for three times. The nanoparticles were dispersed in the aq. ammonia solution (33%, 15 ml) and stirred for overnight at room temperature. The nanoparticles were collected by centrifugation, washed with water followed by acetone and characterized by FT-IR.

2.2.6. Labeling of nanoparticles by FITC for internalization study

The labeling of UCNPs with FITC was done first on amine functionalized UCNPs. Using these nanoparticles, further functionalization with D-glucose or 2-deoxy-D-glucose

moieties was performed. Briefly, the amine functionalized UCNPs (50 mg) were dispersed in dry dimethyl sulphoxide (DMSO, 5 ml). 100 µl of FITC in DMSO (500 µg/ml) was added and stirred for overnight. UCNPs were collected with centrifugation, washed with water and then transferred to dialysis tubing and placed in dialysis buffer containing 0.9 M saline. The buffer was periodically changed after every 12 h till 48 h. The FITC functionalized UCNPs were collected by centrifugation then washed with acetone and dried under reduced pressure.

2.3. Cell culture

MCF-7 cells were procured from Merck Millipore and maintained as monolayer using DMEM media supplemented with 10% fetal bovine serum at 37 °C with 5% CO_2 in a humidified environment. For every experiment, seeding of cells was carried out one day ahead of the experiment.

2.4. Cytotoxicity study by MTT assay

MTT assay was performed in accordance with the standard protocol.[18] Briefly, MCF-7 cells (5000 cells per well) were seeded in a 96-well plate and treated with UCNPs functionalized with D-glucose or 2-deoxy-D-glucose as indicated for 48 h. MTT solution (10 µl; stock solution = 5 mg/ml) was added 3 h prior to addition of DMSO. 100 µl DMSO was added to each well and mixed using a pipette to fully dissolve the formazan crystals. The absorbance was measured at 590 nm using a plate reader.

2.5. Internalization study

MCF-7 cells (5 x 10^5 per well) were seeded in 6-well plate and treated with UCNPs for 12 h. The cells were washed with PBS to remove the trace of UCNPs that were not internalized. The images of the cells were captured using phase contrast microscope in the presence and absence of 980 nm laser irradiation exposure. For flow cytometry studies, MCF-7 cells were treated with UCNPs or UCNPs-2-DG labeled with FITC as indicated. Cells were harvested by trypsinization, washed, fixed with 2% formaldehyde for 20 min and

then stained with Hoechst. Cells were acquired on flow cytometer and analyzed using FlowJo software.[19]

3. Results and Discussion

The $NaYF_4$ based upconversion nanoparticles doped with Tm and Yb, have been synthesized (vide experimental). The percentage of the dopants are 16% ytterbium and 4% thulium of the corresponding yttrium (80%), hence these UCNPs can be as represented by $NaY_{0.8}Yb_{0.16}Tm_{0.4}F_4$ formula (section **2.2.1.**). Their synthesis was done by thermolysis method using oleic acid as the caping agent and 1-octadecene as the solvent. The XRD pattern of synthesized nanoparticles was found to be matching with the standard hexagonal phase (JCPDF 28-1192; Figure 1 A). In the same XRD pattern we observed a broad peak at $2\theta = 20°$ (Figure 1 A) which is attributable to oleic acid. The long chain organic molecules show very broad amorphous peaks in XRD patterns. From literature it is evident that the XRD pattern of the oleic acid coated nanoparticles exhibit this peak and after removing oleic acid, the broad peak corresponding to oleates was not observed.[20] Further, the morphology of the synthesized UCNPs was studied using TEM and the UCNPs were found to be uniform in shape and size. The average size of the nanoparticles is in the range of 24±1 nm with the cuboid shape (Figure 1 B).

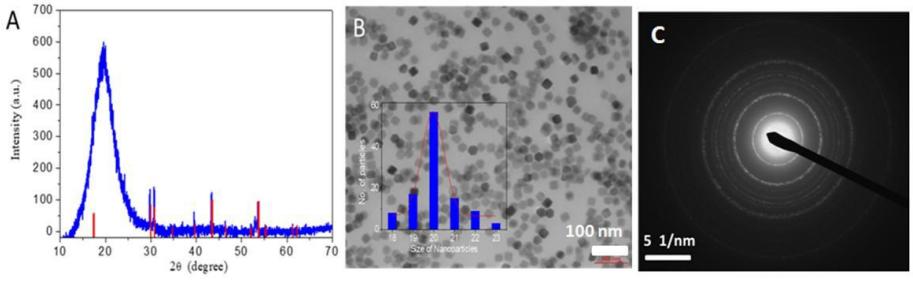

Figure 1. Characterization of $NaYF_4$: Tm, Yb by X-ray diffraction analysis (A), TEM image captured using Jeol TEM (B), the particle distribution (inset B) and Selected area electron diffraction pattern (C).

The selected area electron diffraction pattern further confirmed that the synthesized UCNPs were crystalline (Figure 1 C). As the synthesized nanoparticles were found to be hydrophobic due to the presence of oleic acid on the surface, the nanoparticles were dispersible into the nonpolar solvent like chloroform or hexane. In order to use these nanoparticles for biological applications, the particles should be dispersible in water.[21] In order to make the particles water dispersible, the nanoparticles were coated with silica using tetraethyl orthosilicate and agglomeration was anticipated to be avoided by using IGEPAL CO-520 as the surfactant which helps in formation of uniformly silica coated nanoparticles and avoid the agglomeration. But some aggregation of uniformly silica coated nanoparticles was seen in TEM image (Figure 2 B). The reason for this agglomeration is sonication process or uneven mixing while preparing the sample for TEM. In this process, the interparticle collisions occur under the influence of ultrasonication which leads to agglomeration which results in changing the morphology of the particles.[22] The coating of the nanoparticles with SiO_2 was confirmed by TEM (Figure 2 B). Due to the difference in the refractive index between $NaYF_4$ and SiO_2, the formation of silica layer above $NaYF_4$ was clearly observed. The average size of the nanoparticles ranges between 60-65 nm (Figure 2 C). The thickness of the silica shell is approximately 20-30 nm.

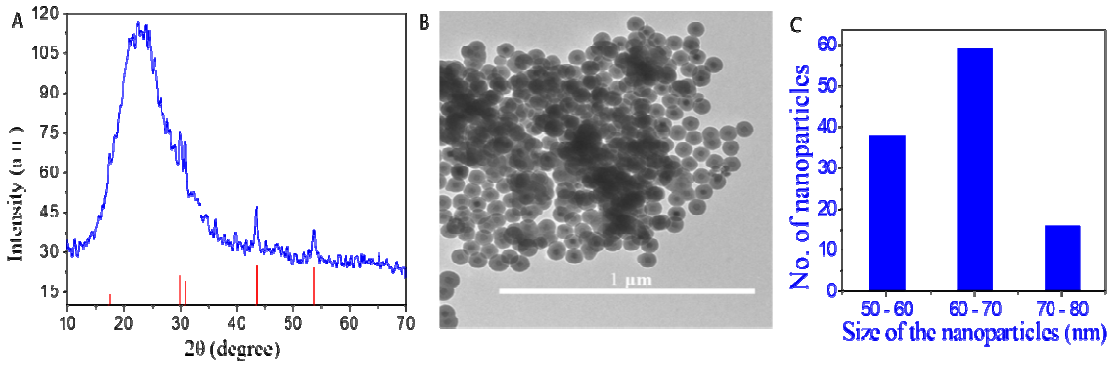

Figure 2. Characterizations of silica coated $NaYF_4$: Tm, Yb UCNPs by XRD (A), TEM (B) and the particle size distribution (C).

View Article Online
DOI: 10.1039/D0NJ00666A

The XRD pattern of $NaYF_4$@SiO_2 is shown in Figure 2 A. The presence of the broad peak centered at around 2θ = 23° which attributes to amorphous silica which also confirms the formation of silica layer on the surface of $NaYF_4$ which is evidenced in the earlier research reports also.[23] Further, the photoluminescence of the synthesized UCNPs was measured with 980 nm laser excitation and the exhibited emission is shown in Figure 3 A. The emission spectra of $NaYF_4$: 16 % Yb, 4 % Tm consists of the blue emission bands at 450.5 and 475 nm which correspond respectively to the $^1G_4 \rightarrow {}^3H_6$ and $^1G_4 \rightarrow {}^3H_6$ transitions of thulium (Figure 3 A). A strong predominant NIR emission at 801.5 nm is attributed to the $^1G_4 \rightarrow {}^3H_5$ transition.[24]

For functionalization of the synthesized UCNPs, amine functional groups were introduced on the surface of UCNPs by treating with (3-aminopropyl)trimethoxysilane (APTMS). The presence of amine functional groups on the surface of the UCNPs after treating with APTMS, was confirmed by the FT-IR spectroscopy which exhibited peaks centered at 1619 cm^{-1} (N-H bend) 3360 cm^{-1} (broad, N-H str.) (Figure 3 B).[25] The obtained amine functionalized UCNPs were stored at 0 °C.

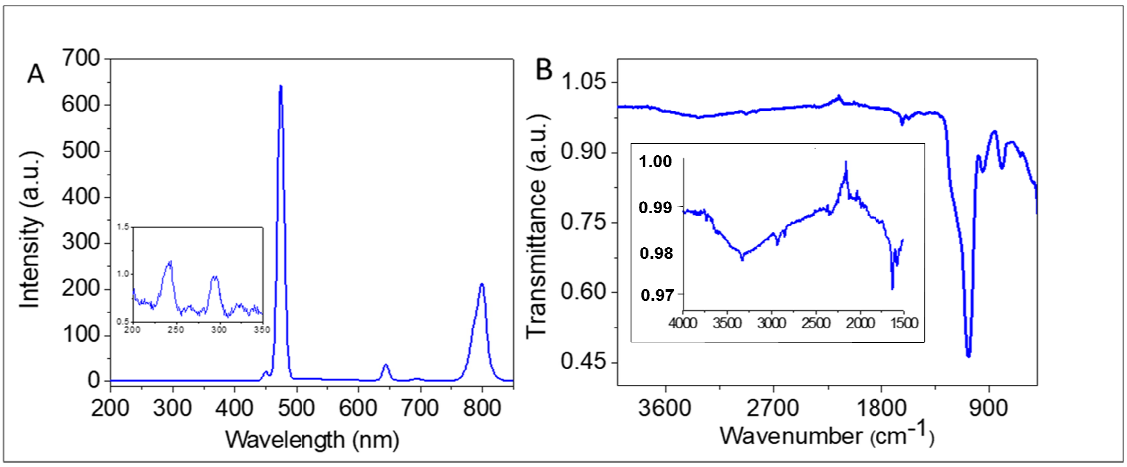

Figure 3. Photoluminescence spectrum of UCNPs with 980 nm laser excitation (A); its expansion (inset A) and FT-IR spectrum of UCNPs: $NaYF_4$: Tm, Yb@SiO_2 functionalized with amine (B); its expansion (inset B)

The synthesis of D-glucose or 2-deoxy-D-glucose compounds was done by either acetylation or benzoylation of the hydroxyl groups of glucose, which made the compound hydrophobic, allowing the reactions to be performed in non-polar organic solvents. Bromination at the acetal carbon (C-1) was done by substitution of the acetyl group. This was confirmed by ^{1}H and $^{13}C\{^{1}H\}$ NMR spectroscopy (*Suppl. Info.* Figure S 1 and S 2). It was observed that the bromo derivatives were very reactive and unstable. The synthesized bromo derivatives were used for next reaction without any further purification.

The bromo-derivative of acetylated glucose was reacted with allyl alcohol using silver carbonate giving allyl glucosides following the reported method. The formation of allyl glucoside was confirmed by ^{1}H and $^{13}C\{^{1}H\}$ NMR spectroscopy (*Suppl. Info.* Figure S 3 and S 4). The terminal double bond of allyl glucoside was converted to carboxylic acid with the loss of a carbon atom, using sodium periodate and ruthenium chloride. The formation of carboxyl glucoside was confirmed by ^{1}H and $^{13}C\{^{1}H\}$ NMR spectroscopy (*Suppl. Info.* Figures S 5 & S 6). The carboxyl group was conjugated with the amine functional groups present on the surface of UCNPs. Using DCC, followed by deacetylation, aq. ammonia solution (30%). The presence of the glucose moiety on the surface of UCNPs was confirmed by FT-IR spectroscopy. In FT-IR spectra, after treating amine functionalized UCNPs with carboxyl glucoside, the peaks at 3320 cm^{-1} for N-H str. of primary amine and 2929 cm^{-1} and 2846 cm^{-1} of C-H str. is suppressed by broad peak of O-H str. centered at 3248 cm^{-1} (Figure 4 A).

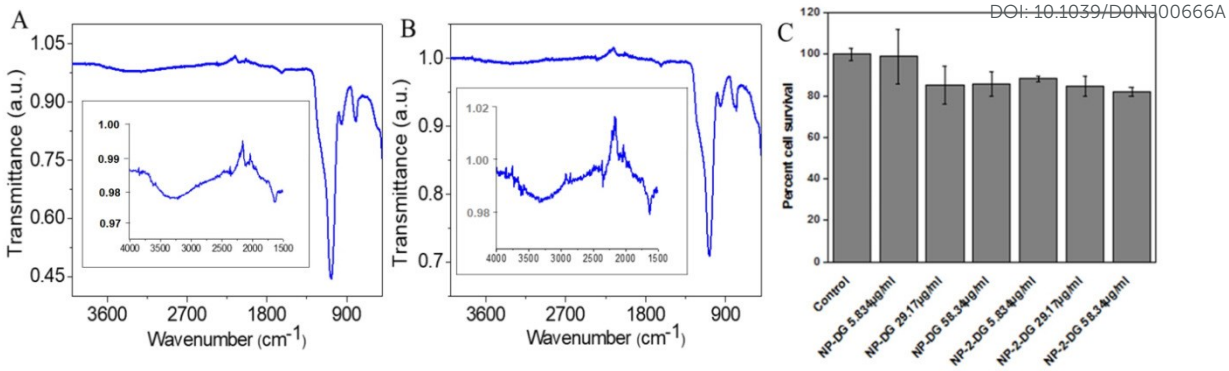

Figure 4. FT-IR spectra of UCNPs: $NaYF_4$: Tm, Yb@ SiO_2 were functionalized with D-glucose (DG) (A); its expansion (inset A) and 2-deoxy-D-glucose (2-DG) (B); its expansion (inset B), MTT assay data (C)

On the other hand, when bromo derivative of acetylated glucose was treated with zinc metal and ammonium chloride, a glycal was formed with the elimination of acetyl group at C-2. When the resultant glycal was treated with acetic acid, acetic anhydride and HBr under an inert Ar atmosphere, 2-deoxy-tetra-acetylglucose was generated. This was subsequently, treated with HBr (33%) in acetic acid to form 2-deoxy-triacetylglucopyranose bromide. This 2-deoxy-triacetylglucopyranose bromide is so reactive that it decomposes with just exposure to normal air. To circumvent that, benzoylation of D-glucose, instead of acetylation, was carried out using benzoyl chloride and pyridine in dried dichloromethane (DCM) and similar procedure for glycal synthesis was performed. The 2-deoxy-tribenzoylglucopyranose bromide obtained was found to be stable enough for recording ^{1}H and $^{13}C\{^{1}H\}$ NMR (*Suppl. Info.* Figure S 13 and S 14) and proceeding to the next reaction.

The 2-deoxy-tribenzoylglucopyranose bromide was reacted with freshly prepared silver thiocyanate formed by reacting silver nitrate and potassium thiocyanate in toluene under reflux. The 2-deoxy-tribenzoyl isothiocyanate formed (*Suppl. Info.* Scheme S 2) was confirmed by ^{1}H and $^{13}C\{^{1}H\}$ NMR (*Suppl. Info.* Figure S 15 and S 16). The 2-deoxy-

tribenzoyl-glucopyranose isothiocyanate was conjugated to the amine functionalized UCNPs in dimethyl formamide (DMF) by heating at 60 °C for 8 h.[26] The 2-deoxy-tribenzoylglucopyranose moiety was attached to the surface of UCNPs via thiourea linkage. The benzoyl protection of 2-DG bound on the surface of UCNPs was removed by treating with aqueous ammonia solution (25%) (Scheme 1). The presence of 2-deoxy-D-glucose moieties on the surface of UCNPs was confirmed by FT-IR (Figure 4 B).

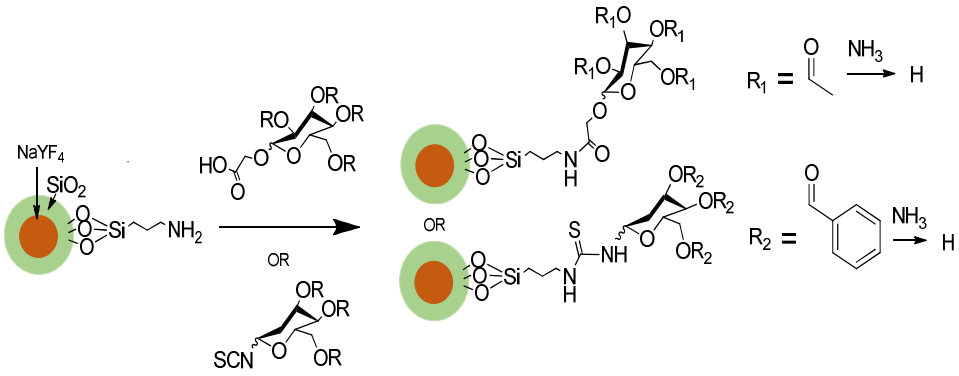

Scheme 1. Functionalization of UCNPs with D-glucose and 2-Deoxy-D-glucose

After functionalization of UCNPs with D-glucose or 2-DG, cytotoxicity was investigated in human mammary cancer cells (MCF-7) using different concentrations for 48 h. The UCNPs functionalized with either D-glucose or 2-DG, showed marginal loss of cell survival as compared to control (Figure 4 C).

Cellular internalization of UCNPs was studied by microscopy and flow cytometry using MCF-7 cells. The cells were seeded in 6-well plate and treated with or without UCNPs for 12 h. Cells were washed with PBS and observed under microscope. The images were captured in phase contrast mode or in the presence of 980 nm laser. As the concentration of UCNPs increased from 29.17 µg/ml to 58.34 µg/ml the emission of UCNPs at blue region also increased indicating the internalization of UCNPs by MCF-7 cells (Figure 5).

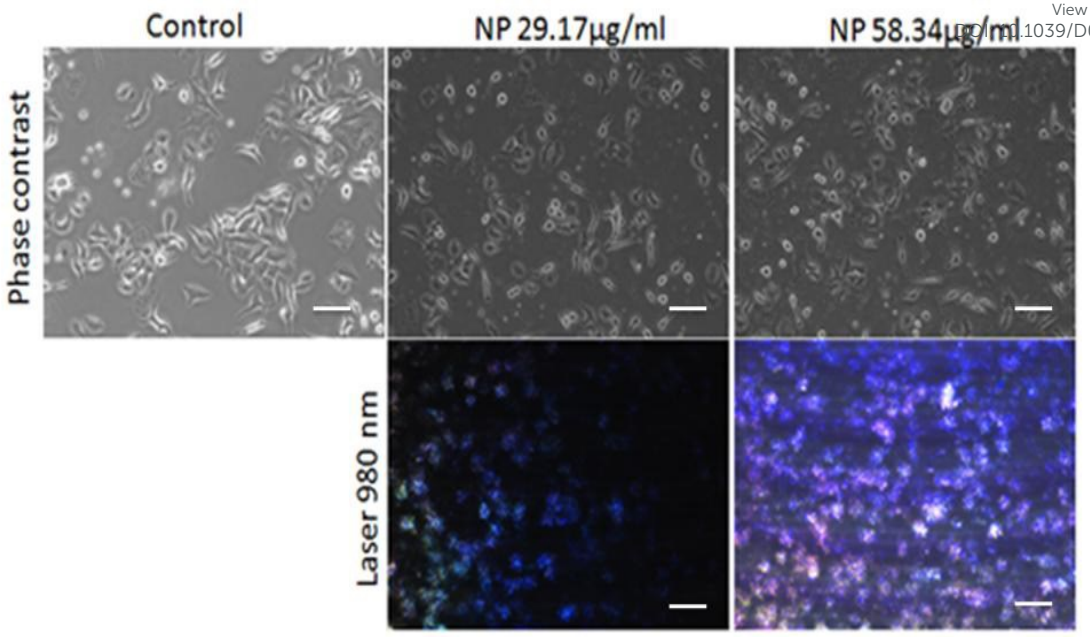

Figure 5. UCNPs internalization studies: MCF-7 cells (0.2 x 10^6) were seeded in 6-well plate and then treated with UCNPs for 12 h. Cells were washed with PBS and images were taken using phase contrast microscope with or without exposure to 980 nm laser. Scale bar = 50 µm.

Labeling of FITC was done on amine functionalized UCNPs and these nanoparticles were further functionalized with 2-DG moieties on the amine groups. MCF-7 cells were grown in glucose free media for overnight and treated UCNPs-FITC or UCNPs-2-DG for 10 min, 1 h, 3 h and 6 h. Cells were washed and harvested by trypsinization. Harvested cells were fixed with 2% paraformaldehyde and then stained with Hoechst 33342. Increase in the FITC fluorescence was used as the criteria for internalization of UCNPs by MCF-7 cells. The percentage of UCNPs internalization was analyzed by using FlowJo software. Functionalization of UCNPs with 2-DG significantly increased the uptake of nanoparticles in glucose starved MCF-7 cells at all time points (Figure 6 A and 6 B). The uptake UCNPs by MCF-7 is a time dependent and slow process, but the uptake of UCNPs-2-DG is rapid and nearly 53% uptake of UCNPs-2-DG is seen within 10 min incubation and 83% after 1 h.

View Article Online
DOI: 10.1039/D0NJ00666A

These results clearly demonstrated the following two advantages of using UCNPs-2-DG during cancer treatment. They are taken up by tumor cells easily and UCNPs give luminescence when exposed to 980 nm laser thereby distinguishing between the tumor and normal cells.

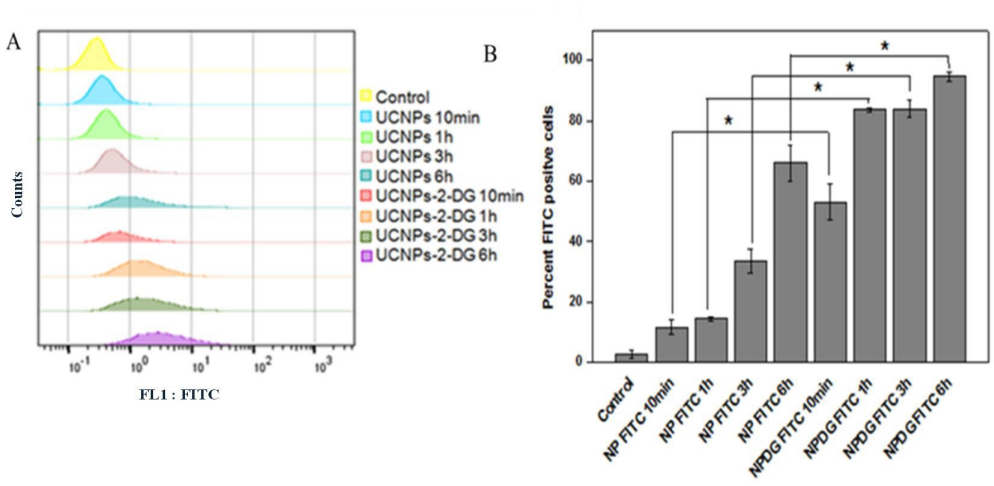

Figure 6. MCF-7 cells were cultured in D-glucose free media and treated with FITC labeled UCNPs functionalized with or without 2-Deoxy-D-glucose (2-DG). MCF-7 cells were stained with Hoechst 33342 and acquired on a flow cytometer. The samples were analyzed using FlowJo software (A) and bar graph represents the percentage of FITC positive cells (B).

Now it is well known fact that the uptake of D-glucose by cancer cells is twenty-fold higher than that of the normal cells.[15] Also literature reports, regarding comparison of D-Glucose and 2-DG uptake clearly indicate that the 2-deoxy-D-glucose (2-DG) has ability to compete with D-glucose uptake and inhibit its metabolism in tumor cells as well as non-tumor cells. Preferential and fast uptake kinetics of 2-DG leads to deprivation of nutrient and energy resulting in suppress cancer cell growth and survival and leading to their death through apoptotic pathway.[27] The 2-deoxy-D-glucose that is functionalized with the UCNPs are

anticipated to get released under acidic conditions upon internalization by cells. The 2-deoxy-D-glucose mimics D-glucose and blocks the glycolysis pathway. Finally UCNPs have advantage over fluorophores due to zero auto fluorescence and are resistant to photo bleaching which make them suitable for long term repetitive imaging. Hence, UCNPs-2-DG can act as multipurpose drug in diagnosis and therapy by further increasing the ability of UCNPs to take more load of 2-deoxy-D-glucose or tag with known chemotherapeutic agent.

At this point it is worthy to note that during the anticipated clinical applications of this modality, the exposure of to 980 nm will not cause any harm to tissues due to its low energy (1-4 mW/cm^{-2}) and short duration of exposure of few seconds. Its tissue penetration is also more than the medically used red light radiation. At present the lasers have been used in versatile medical applications especially super facial applications, lithotripsy, for the treatment of various types of cancer and surgery too.[28] Additionally, it is now known that water is a major component of tissue. Its absorption coefficient at 980 nm is 0.482 cm^{-1} (better as compared at other wavelengths of available lasers) which directly proportional to optical thermal generation in tissue. Hence the 980 nm diode laser is capable of producing rapid and localized heating of tissue and thereby creating ablation zones with sharp boundaries using relatively low powers of incident laser radiation.[29] It is helpful for serving our purpose for application of this modality for precision surgery.

The conclusion of this present study will be incomplete without proposing the pathway of observed functions exhibited by D-Glucose or 2-DG coated UCNPs *viz.,* internalization and cytotoxicity. It may perhaps give directive for further research. For this we need to go through the difference in D-Glucose metabolism in cancerous as well as normal cells. From literature it is evident that in case of normal cells, through glycolysis and oxidative phosphorylation, mammalian cells get ATP and precursors of amino acids, nucleotide and lipids using D-glucose as the precursor. The transport of D-glucose into the

cytosol through the plasma membrane is a rate-limiting step in this glucose metabolism. This transport of D-glucose is performed by a family of glucose transporters (GLUTs) proteins expressed in tissues. One of the most important GLUTs is GLUT-1. But, in case of cancerous cells different scenario is seen. The cancer cells depend preferably on glycolysis (2 ATP per glucose) which is contrast to normal cells that metabolize glucose through oxidative phosphorylation (36 ATP per glucose) and resort to the glycolytic pathway under anaerobic conditions. This anaerobic glycolysis (Warburg Effect) entails the generation of lactate and is also found to be far less efficient than mitochondrial respiration. As cancer cells rely on glycolysis, the demand of glucose is twenty fold higher than of normal cells. This leads to the over expression of GLUT-1 on the surface of the cancer cells. This has lead the successful treatment of 2-DG which is an antimetabolite of D-Glucose responsible for killing cancer cells by inhibiting glycolysis.[30] Analogously, when the cancer cells were treated with 2-DG coated UCNPs, the UCNPs interact with GLUT-1 transporters present on the surface of the cancer cells and eventually get internalized inside the cells through clathrin-mediated endocytosis mechanism and perform their function. Once the 2-DG is released, it inhibits the glycolysis leading to death of cancer cell.

4. Conclusions

Monodispersed UCNPs based on $NaYF_4$ doped with Yb (16%) and Tm (4%) with the hexagonal phase were prepared which exhibited luminescence upon exposure to 980 nm laser. To make these UCNPs, hydrophilic, uniform silica coating was performed and subsequently functionalized with D-glucose or 2-deoxy-D-glucose. UCNPs functionalized with 2-deoxy-D-glucose were found to have enhanced uptake by MCF-7 human breast cancer cells and they are anticipated to inhibit growth by mimicking the glucose, thereby blocking the glycolysis pathway, resulted in killing of MCF-7 cells. Then we labeled UCNPs coated

with 2-deoxy-D-glucose with FITC and faster uptake (80 %) within 30 min was confirmed by flow cytometer and internalization studies. Hence, we conclude with possible application of 2-DG coated UCNPs for targeted delivery as well as in precision surgery.

5. Supplementary Information

† Electronic supplementary information (ESI) is available: Some experimental details related synthesis of D-glucose, 2-deoxy-D-glucose derivatives as well as their characterization data by NMR (^{1}H. ^{13}C{^{1}H}) spectroscopy is given in supplementary information.

6. Acknowledgements

Authors are thankful Dr. A. K. Tyagi, Head, Chemistry Division, BARC, Trombay, Mumbai for the encouragement and support for this research work. Authors also acknowledge the fruitful discussions with Dr. R. S. Ningthoujam, Chemistry Division, BARC as well as Dr. Dibakar Goswami, Bio-Organic Division, BARC. We are thankful to Ms. Binita Kislay Kumar and Mr. Deepak V. Kathole for technical assistance during conducting biological experiments. KSS is grateful to University Grants Commission (UGC), New Delhi for the award of fellowship.

View Article Online
DOI: 10.1039/D0NJ00666A

Author information

Affiliations

Chemistry Division, Bhabha Atomic Research Centre, Mumbai, 400 085, India

K. Shitaljit Sharma

Chemistry Division, Bhabha Atomic Research Centre, Mumbai, 400 085, India & Homi Bhabha National Institute, Anushaktinagar, Mumbai-400 094, India

Prasad P. Phadnis and Rajesh K. Vatsa

Bio-organic Division, Bhabha Atomic Research Centre, Mumbai, 400 085, India

Akhil K. Dubey

Radiation Biology & Health Sciences Division, Bhabha Atomic Research Centre, Mumbai-400 085, India

Maikho Thoh

Radiation Biology & Health Sciences Division, Bhabha Atomic Research Centre, Mumbai 400085, India & Homi Bhabha National Institute, Anushaktinagar, Mumbai-400 094, India

Deepak Sharma and Santosh K. Sandur

Corresponding authors

Correspondence to: Dr. Prasad P. Phadnis; Dr. Rajesh K. Vatsa

Email: phadnisp@barc.gov.in; rkvatsa@barc.gov.in

View Article Online
DOI: 10.1039/D0NJ00666A

Author Contributions

KSS and PPP designed the work and performed synthesis of silica coated $NaYF_4$ and its functionalization with D-glucose and 2-deoxy-D-glucose. KSS, AKD and PPP conducted the synthesis of D-glucose or 2-DG derivatives and their functionalization over upconversion nanoparticles (UCNPs) to give UCNPs-D-Glucose and UNCPs-2-deoxy-D-glucose respectively. MT, DS and KSS performed cell viability evaluation by treatment of UCNPs-D-Glucose and UNCPs-2-deoxy-D-glucose against MCF-7 cells by MTT assay. KSS and MT performed the biological experiments. DS, MT and KSS performed imaging and internalization studies. PPP and KSS analyzed and concluded NMR spectral analyses. KSS, PPP, MT and RKV wrote the manuscript. PPP and KSS analyzed and concluded NMR spectral analyses. RKV supervised overall work.

Ethics declarations

Conflicts of interest

"There are no conflicts to declare".

References

1. (a) F. Auzel, *Chem. Rev.,* 2004, **104**, 139-173; (b) K. Binnemans, *Chem. Rev.,* 2009, **109**, 4283-4374.

2. (a) E.-K. Lim, T. Kim, S. Paik, S. Haam, Y.-M. Huh and K. Lee, *Chem. Rev.,* 2015, **115**, 327-394; (b) S. F. Lim, R. Riehn, W. S. Ryu, N. Khanarian, C.-k. Tung, D. Tank and R. H. Austin, *Nano Lett.*, 2006, **6**, 169-174.

3. (a) J. Zhou, Z. Liu and F. Li, *Chem. Soc. Rev.*, 2012, **41**, 1323-1349; (b) G. Chen, I. Roy, C. Yang and P. N. Prasad, *Chem. Rev.*, 2016, **116**, 2826-2885; (c) B. R. Smith and S. S. Gambhir, *Chem. Rev.*, 2017, **117***,* 901-986.

4. (a) G. Chen, H. Qiu, P. N. Prasad and X. Chen, *Chem. Rev.*, 2014, **114**, 5161-5214; (b) M. Wang, C.-C. Mi, W.-X. Wang, C.-H. Liu, Y.-F. Wu, Z.-R. Xu, C.-B. Mao and S.-K. Xu, *ACS Nano*, 2009, **3**, 1580-1586; (c) A. B. Chinen, C. M. Guan, J. R. Ferrer, S. N. Barnaby, T. J. Merkel and C. A. Mirkin, *Chem. Rev.*, 2015, **115**, 10530-10574.

5. (a) L. Cheng, K. Yang, Y. Li, J. Chen, C. Wang, M. Shao, S.-T. Lee and Z. Liu, *Angew. Chem. Int. Ed. Engl.*, 2011, **50***,* 7385-7390; (b) M. Lin, Y. Zhao, SQ. Wang, M. Liu, ZF. Duan, YM. Chen, F. Li, F. Xu and TJ. Lu, *Biotechnol. Adv.*, 2012, **30**, 1551-1561; (c) J. Shen, L. Zhao and G. Han, *Adv. Drug Deliv. Rev.*, 2013, **65***,* 744-755.

6. (a) S. S. Lucky, K. C. Soo and Y. Zhang, *Chem. Rev.*, 2015, **115**, 1990-2042; (b) G. Chen, J. Shen, T. Y. Ohulchanskyy, N. J. Patel, A. Kutikov, Z. Li, J. Song, R. K. Pandey, H. Ågren, P. N. Prasad and G. Han, *ACS Nano*, 2012, **6**, 8280-8287.

7. (a) N. Erathodiyil and J. Y. Ying, *Acc. Chem. Res.*, 2011, **44**, 925-935; (b) J. Yao, M. Yang and Y. Duan, *Chem. Rev.*, 2014, **114**, 6130-6178.

8. (a) L. J. Kleinsmith, *Principles of Cancer Biology*, Pearson Benjamin Cummings: San Francisco: Pearson Benjamin Cummings, 2006; (b) M. A. Knowles, *Introduction to the*

Cellular and Molecular Biology of Cancer, Oxford University Press Inc., New York, 2005.

9. (a) M. A. Richards, A. M. Westcombe, S. B. Love, P. Littlejohns and A. J. Ramirez, *Lancet*, 1999, **353**, 1119-1126; (b) K. M. Reid, A. Ramos-De la Medina and J. H. Donohue, *J. Gastrointest. Surg.*, 2007, **11**, 671-681.
10. L. Sun, R. Legood, I. Dos-Santos-Silva, S. M. Gaiha and Z. Sadique, *PLoS One*, 2018, **13 (11)**, e0207993.
11. B. M. Fischer, J. Mortensen and L. Højgaard, *Lancet Oncol.*, 2001, **2**, 659-666.
12. (a) X. Yu, X. Li, X. Song, D. Dai, L. Zhu, Y. Zhu, J. Wang, H. Zhao and W. Xu, *Oncol. Lett.*, 2016, **12**, 3785-3792; (b) I. Kantorová, L. Lipská, O. Bêlohlávek, V. Visokai, M. Trubaĉ and M. Schneiderová, *J. Nucl. Med.*, 2003, **44**, 1784-1748.
13. K. N. Syrigos, D. Karachalios, E. M. Karapanagiotou, C. M. Nutting, L. Manolopoulos and K. J. Harrington, *Cancer. Treat. Rev.*, 2009, **35**, 237-245.
14. A. Urruticoechea, R. Alemany, J. Balart, A. Villanueva, F. Viñals and G. Capellá, *Curr. Pharm. Des.*, 2010, **16**, 3-10.
15. M. G. V. Heiden, L. C. Cantley and C. B. Thompson, *Science*, 2009, **324**, 1029-1033.
16. (a) M. C. Parrott, M. Finniss, J. C. Luft, A. Pandya, A. Gullapalli, M. E. Napier and J. M. DeSimone, *J. Am. Chem. Soc.*, 2012, **134**, 7978-7982; (b) Y. Yan, J. Fu, T. Wang and X. Lu, *Acta. Biomater.*, 2017, **51**, 471-478; (c) J. B. Lee, A. Zgair, J. Malec, T. H. Kim, M. G. Kim, J. Ali, C. Qin, W. Feng, M. Chiang, X. Gao, G. Voronin, A. E. Garces, C. L. Lau, T. H. Chan, A. Hume, T. M. McIntosh, F. Soukarieh, M. Al-Hayali, E. Cipolla, H. M. Collins, D. M. Heery, B. S. Shin, S. D. Yoo, L. Kagan, M. J. Stocks, T. D. Bradshaw, P. M. Fischer and P. Gershkovich, *J. Control Release*, 2018, **286**, 10-19; (d) M. C. Parrott, J. C. Luft, J. D. Byrne, J. H. Fain, M. E. Napier and J. M.

DeSimone, *J. Am. Chem. Soc.*, 2010, **132**, 17928-17932; (e) L. D. Lavis, *ACS Chem. Biol.*, 2008, **3**, 203-206.

17. (a) Fu. Zhang, C.-L. Zhang, H.-Y. Peng, H.-P. Cong and H.-S. Qian, *Part. Part. Syst. Charact.*, 2016, **33**, 248-253; (b) F. Zhang, C.-L. Zhang, W.-N. Wang, H.-P. Cong and H.-S. Qian, *ChemSusChem.*, 2016, **9**, 1449-1454; (c) W.-N. Wang, C.-X. Huang, C.-Y. Zhang, M.-L. Zhao, J. Zhang, H.-J. Chen, Z.-B. Zha, T. Zhao, H.-S. Qian, *Applied Catalysis B: Environmental*, 2018, **224**, 854-862; (d) B.-B. Ding, H.-Y. Peng, H.-S. Qian, L. Zheng and S.-H. Yu, *Adv. Mater. Interfaces*, 2016, **3**, 1500649.

18. G. Ciapetti, E. Cmni, L. Pratelli and A. Pizzoferrato, *Biomaterials*, 1993, **14**, 359-364; T. Mossmann, *J. Immunol. Methods*, 1983, **65**, 55-63.

19. M. Thoh, R. S. Patwardhan, T. N. Das, D. Sharma and S. K. Sandur, *Free Radic. Res.*, 2018, **52**, 212-222.

20. (a) S. Sun and H. Zeng, *J. Am. Chem. Soc.*, 2002, 124, 8205-8205; (b) K. S. Sharma, R. S. Ningthoujam, A. K. Dubey, A. Chattopadhyay, S. Phapale, R. R. Juluri, S. Mukherjee, R. Tewari, N. G. Shetake, B. N. Pandey and R. K. Vatsa, *Sci. Rep.*, 2018, 8, Article number: 14766 (P 1-11).

21. (a) T. L. Moore, L. Rodriguez-Lorenzo, V. Hirsch, S. Balog, D. Urban, C. Jud, B. Rothen-Rutishauser, M. Lattuada and A. Petri-Fink, *Chem. Soc. Rev.*, 2015, **44**, 6287-6305; (b) C. Fang, N. Bhattarai, C. Sun and M. Zhang, *Small*, 2009, **5**, 1637-1641.

22. (a) S. J. Doicrycz and K. S. Suslick, *Science*, 1990, **247**, 1067-1069; (b) S. Santra, R. Tapec, N. Theodoropoulou, J. Dobson, A. Hebard and W. Tan, *Langmuir*, 2001, **17**, 2900-2906.

23. (a) S. Xu, Y. Yu, Y. Gao, Y. Zhang, X. Li, J. Zhang, Y. Wang and B. Chen, *Microchim. Acta*, 2018, **185,** Article No, 454 (1-10 pages); (b) C. Kembuan, M. Saleh,

B. Rühle, U. Resch-Genger and C. Graf, *Beilstein J. Nanotechnol.*, 2019, **10**, 2410-2421.

24. (a) J. C. Zhou, Z. L. Yang, W. Dong, R. J. Tang, L. D. Sun and C. H. Yan, *Biomaterials* 2011, **32**, 9059-9067; (b) G.-S. Yi and G.-M. Chow, *Chem. Mater.*, 2007, **19**, 341-343.

25. D. L. Pavia, G. M. Lampman, G. S. Kriz and J. R. Vyvyan, *Introduction to spectroscopy*, Brook/cole Cengage learning, 2009.

26. C. Saitz-Barria, A. Torres-Pinedo and F. Santoyo-González, *Synlett*, 1999, **12**, 1891-1894.

27. (a) B. Pajak, E. Siwiak, M. Sołtyka, A. Priebe, R. Zieliński, I. Fokt, M. Ziemniak, A. Jaśkiewicz, R. Borowski, T. Domoradzki and W. Priebe, *Int. J. Mol. Sci.*, 2020, **21**, 234; (b) K. B. Philips, M. Kurtoglu, H. J. Leung, H. Liu, N. Gao, M. A. Lehrman, T. G. Murray and T. J. Lampidis, *Cancer Chemother. Pharmacol.*, 2014, **73**, 349-361; (c) J. C. Maher, M. Wangpaichitr, N. Savaraj, M. Kurtoglu and T. J. Lampidis, *Mol. Cancer Ther.*, 2007, **6**, 732-741; (d) A. E. M. Jacobs, A. Oosterhof and J. H. Veerkamp, *Biochlmica et Biophvsica Acta*, 1990, **1051**, 230 -236; (e) T. Doenst and H. Taegtmeyer, *J. NucI. Med.*, 2000, **41**, 488-492; (f) J. P. Bader, N. R. Brown and D. A. Ray, *Cancer. Res.*, 1981, **41**, 1702-1709; (g) B. S. Dwarakanath and V. Jain, *Future Oncol.,* 5 (2009) 581-585; (h) M. Taghikhani, L. W. Lavi, P. G. Woost and C. C. Griffin, *Biochimica et Biophysica Acta (BBA) - Molecular Cell Research,* 1984, **803**, 278-283.

28. (a) M. Wehner, P. Betz and M. Aden, *Laser Med. Sci.*, 2019, **34**, 335-341;(b) B. Azadgoli, R. Y. Baker, *Ann. Transl. Med.*, 2016, **4**, 452 (1-7 pages); (c) A. Desiate, S. Cantore, D. Tullo, G. Profeta, F. R. Grassi and A. Ballini, *Int. J. Med. Sci.*, 2009, **6**, 358-364; (d) T. N Aldelaimi and A. A Khalil, *J. Craniofac, Surg.*, 2015, **26**, 1220-1223; (e) H. H. Arroyo, L. Neri, C. Y. Fussuma, R. Imamura, *Int. Arch. Otorhinolaryngol.*,

2016, **20**,172-179; (f) T. Ma,Y.-C. Chai, H.-Y. Zhu, H. Chen, Y. Wang, Q.-S. Li, L.-H. Pang, R.-Q. Wu, Y. Lv, D.-H. Dong, *Lasers Surg. Med.,* 2019, **51**, 720-726; (g) O. Bozkulak, H. O. Tabakoglu, A. Aksoy, O. Kurtkaya, A. Sav, R. Canbeyli and M. Gulsoy, *Laser Med. Sci.*, 2004, **19**, 41-47; (h) D. E. Hudson, .D. O. Hudson, J. M. Wininger and B. D. Richardson, *Photomed. Laser Surg.*, 2013, **31**, 163-168.

29. (a) K. Ahrar, A. Gowda, S. Javadi, A. Borne, M. Fox, R. McNichols, J. U. Ahrar, C. Stephens and R. J. Stafford, *J. Vasc. Interv. Radiol.*, 2010, **21**, 555-561.

30. (a) Chan Y. Jung, *Exp. Mol. Med.*, 1996, **28**, 153-160; (b) A. M. Navale and A. N. Paranjape, *Biophys. Rev.*, 2016, **8**, 5-9; (c) G. D. Holman, *Biochem J.*, 2018, **475**, 3511-3534; (d) G. K. Brown, *J. Inherit. Metab. Dis.*, 2000, **23**, 237-246; (e) X. Fu, G. Zhang, R. Liu, J. Wei, D. Zhang-Negrerie, X. Jian and Q. Gao, *J. Chem. Inf. Model.*, 2016, **56**, 517-526; (f) Y.-C. Yeh, S.T. Kim, R. Tang, B. Yan and V. M. Rotello*, J Mater Chem B Mater Biol Med.*, 2014; **2**,4610-4614; (g) X. Li, M. Bao, Y. Weng, K. Yang, W. Zhang and G. Chen, *J. Mater. Chem. B*, 2014, **2**, 5569-5575; (h) R. Gromnicova, H. A. Davies, P. Sreekanthreddy, I. A. Romero, T. Lund, I. M. Roitt, J. B. Phillips and D. K. Male, *PLoS ONE*, 2013, **8**, e81043 (1-10 pages); (i) C. D. Fahrenholtz, M. Hadimani, S. B. King, S. V. Torti and R. Singh, *Nanomedicine (Lond.)*, 2015, **10**, 2481-2497; (j) J. L. Vivero Escoto, I. I. Slowing, B. G. Trewyn and V. S.-Y. Lin, *small*, 2010, **6**, 1952-1967; (k) Z. Li, H. Guo, H. Qian and Y. Hu, *Nanotechnology*, 2010, **21**, Article no.315105 (1-7 pages); (l) A. Gnach, T. Lipinski, A. Bednarkiewicz, J. Rybka and John A. Capobianco. *Chem. Soc. Rev.*, 2015, **44**, 1561-1584.

View Article Online
DOI: 10.1039/D0NJ00666A

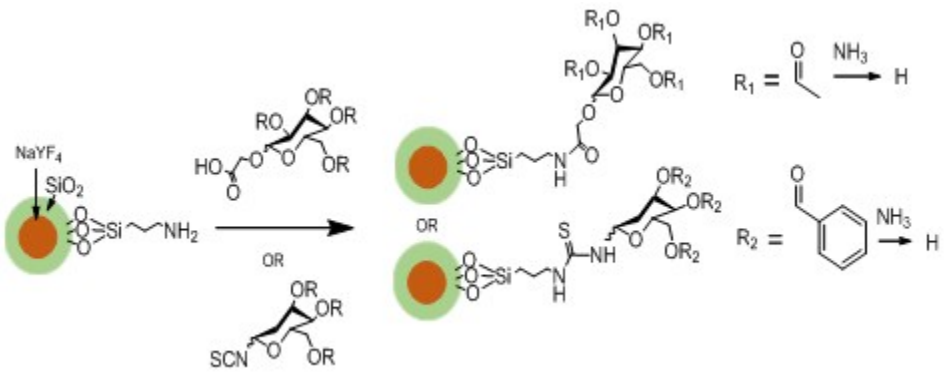

127x52mm (96 x 96 DPI)